NANO LETTERS

Letter

pubs.acs.org/NanoLett

Terms of Use

Fine Tuning and Efficient T Cell Activation with Stimulatory aCD3 Nanoarrays

Jovana Matic,[†,‡] Janosch Deeg,[†,‡] Alexander Scheffold,[§,∥] Itamar Goldstein,[⊥,¶] and Joachim P. Spatz*[,†,‡]

[†]Department of New Materials and Biosystems, Max Planck Institute for Intelligent Systems, Heisenbergstrasse 3, 70569 Stuttgart, Germany

[‡]Department of Biophysical Chemistry, University of Heidelberg, INF 253, Germany

[§]Department of Cellular Immunology, Clinics for Rheumatology and Clinical Immunology, Charité University Medicine Berlin, Berlin, Germany

[∥]German Rheumatism Research Centre (DRFZ) Berlin, Leibniz Association, Berlin, Germany

[⊥]Immunology Core Laboratory, Sheba Cancer Research Center, Chaim Sheba Medical Center, Tel Hashomer 52621, Israel

[¶]Sackler Faculty of Medicine, Tel Aviv University, Israel

Supporting Information

ABSTRACT: Anti-CD3 (aCD3) nanoarrays fabricated by self-assembled nanopatterning combined with site-directed protein immobilization techniques represent a novel T cell stimulatory platform that allows tight control over ligand orientation and surface density. Here, we show that activation of primary human CD4+ T cells, defined by CD69 upregulation, IL-2 production and cell proliferation, correlates with aCD3 density on nanoarrays. Immobilization of aCD3 through nanopatterning had two effects: cell activation was significantly higher on these surfaces than on aCD3-coated plastics and allowed unprecedented fine-tuning of T cell response.

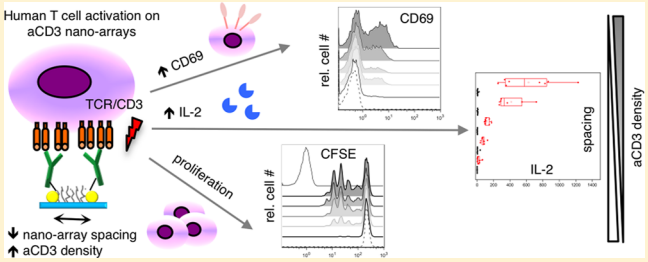

KEYWORDS: *Artificial antigen presenting interfaces, nanopattern, block copolymer micellar nanolithography (BCML), T cell activation, CD4+ T cells, anti-CD3 monoclonal antibody*

Adoptive cell therapy (ACT) is a promising medical strategy for the treatment of cancer and chronic viral infections by transfusion of ex vivo generated T lymphocytes.[1] Essential to this approach is the generation of large numbers of functional T cells to improve the patient's quantitative and qualitative immune response. Developing culture platforms for ex vivo T cell activation and expansion is therefore of particular interest.[2] In vivo, T cell activation occurs through a process where a T cell receptor (TCR) recognizes a cognate peptide-major histocompatibility complex (pMHC) on the surface of antigen presenting cells (APCs).[3] This interaction triggers a complex intracellular signaling network, which finally results in cytokine production (e.g., IL-2), cell proliferation, and differentiation into distinct subsets.[4] Using autologous APCs as T cell stimulatory platforms in vitro is difficult to implement in practice due to great variations in the amount and quality of suitable cells. Artificial APCs have emerged as an easier-to-reproduce and economically more viable system than their natural counterparts and a vast array of cell-based and acellular systems has been engineered for use as APC surrogates.[5,6] Artificial antigen presentation on synthetic substrates such as liposomes and latex or magnetic beads,[7] as well as biodegradable polymers[8] and even water-in-oil emulsion droplets,[9] offers great flexibility and modularity in tailoring the desired stimulatory surface.[7] Synthetic surfaces are, clearly, a very simplified model of a complex cellular interface but have the advantage of allowing key parameters like ligand composition and density to be readily varied for the systematic examination of their effects on T cell response.[10] Minimal molecular input for efficient T cell stimulation depends on the T cell type and state. Usually, it requires both TCR ligation by cognate pMHC as well as a costimulatory signal via the CD28 receptor when it ligates with CD80 and CD86 molecules on APCs.[11] Recent investigations using single cell force spectroscopy showed adhesive interactions between the LFA-1 integrin on T cells and ICAM-1 on APCs to be the main receptor–ligand pair determining force development in this system.[12] This interaction is important for strengthening the contact and for further amplifying the effect of TCR stimulation and costimulatory molecules.[5] Agonistic antibodies to CD3 (a signal transduction component of the TCR complex) and CD28 are often used as mimics of natural ligands for T cell activation and expansion systems. Although antibodies deliver much stronger signals than physiological ligands, there are also

Received: June 20, 2013
Revised: October 3, 2013
Published: October 10, 2013

 © 2013 American Chemical Society dx.doi.org/10.1021/nl4022623 | *Nano Lett.* 2013, 13, 5090–5097

a few advantages to their use for in vitro T cell activation. Anti-CD3 monoclonal antibodies (aCD3 mAbs) trigger highly robust polyclonal T cell activation, as opposed to cognate antigens that trigger only a selective pMHC-restricted oligoclonal response. This response is less efficient for the rapid in vitro expansion of T cells. Anti-CD28 mAbs (aCD28), unlike the natural CD28 ligands, do not bind to the inhibitory receptor CTLA-4, thus avoiding negative regulation of T cell activation and expansion in vitro.

While many studies regarding artificial APC systems have focused on the type of molecular signals needed for the induction or expansion of a specific T cell phenotype, little attention has been given to achieving a desired coupling chemistry and the precise control over ligand density on the surface. The density and number of TCR ligands, alongside other factors like ligand affinity, presence and type of costimulatory molecules and the cytokine milieu,[13] determine the overall signal strength delivered to T cells.[14] Signal strength has a profound impact on T cell fate: signals that are too weak render the cells "unfit" or anergic, while very strong signals can cause cell deletion via activation induced cell death (AICD).[13,15] Intermediate signals of a lower or higher level have a tendency to generate a memory or effector phenotype, respectively.[15b,16] A weak TCR signal causes the induction of Th2[17] and Th17 subsets[18] as well as regulatory T cells,[19] while stronger stimulation predominately results in a Th1 cell phenotype.[20] Depending on the delivered signal, T cells develop different proliferative capacity, effector functions, and homing patterns; all of these being crucial parameters for the effectiveness of adoptive cellular immunotherapy.[21] An APC surrogate that has tight control over ligand orientation and surface density could fine-tune T cell responses by high-quality, stimulating antibody presentation at the interface. Because the number of functional stimulatory ligands impacts T cell fate at various levels, such an artificial APC platform may contribute greatly to the generation of specific T cell subsets and the standardization of rapid expansion protocols for ACT.

Elegant work with supported lipid bilayers that contain physical barriers to restrict the mobility of incorporated molecules revealed that the microscale arrangement of ligands can also affect T cell signaling and activation.[22] Preclustering of TCR ligands (together with costimulatory and adhesion molecules) in microdomains on liposome membranes[23] or on chemically treated carbon nanotubes that allow aCD3 microcluster formation[24] was shown to enhance T cell activation and expansion. Patterns of aCD3 and aCD28 immobilized on solid supports, thereby imposing a permanently attached and stationary microgeometry on T cells, have also underscored the importance of the microscale spatial arrangement of presented molecules for regulating T cell activation.[25] The recent discovery of pre-existing TCR nanoclusters on the plasma membrane of resting T cells[26] has raised interest about the possible roles of nanoscale arrangements of signaling proteins in modulating T cell function.

This study presents a novel nanoarray-based stimulatory platform for T cells. On these arrays aCD3 (anti-TCR complex antibody) is immobilized on gold nanoparticles (AuNPs) in an orientated, bioactive manner and its surface density is finely adjusted by varying the interparticle distance. Nanoarrays are fabricated by block copolymer micellar nanolithography (BCML), a self-assembly technique enabling relatively fast nanopatterning of large surface areas, which presents an advantage for large-scale clinical applications. In the past, such nanoarrays functionalized with relevant ligands have been employed to investigate various processes in other fields of cell biology, such as cell adhesion,[27] neurite growth,[28] and death receptor triggering.[29] In our system, costimulation requirements were met by adding soluble aCD28 with the possibility for coimmobilization on the surface in future experiments. We tested the stimulatory potential of these aCD3 nanoarrays on human CD4+ T cells, as they are postulated to control the adaptive immune response and considered important cellular candidates in HIV and cancer therapy.[30] Monitoring of several short-term and long-term indicators of cellular activation, namely CD69 upregulation, IL-2 secretion and cell proliferation, provided proof-of-concept that such substrates can finely regulate T cell stimulation and maybe even effector functions. These findings can contribute to the development of platforms for ex vivo T cell manipulation for ACT.

Precise and orientated immobilization of molecules on the nanoscale, which translates into fine-tuning the global ligand density, can optimize the stimulatory potential of a surface by minimizing steric hindrance and unfavorable ligand orientation. Relevant biological length scales in receptor−ligand interactions and receptor clustering can be addressed by defining their position on the nanoscale. We used AuNPs hexagonally ordered on glass substrates as anchoring points for the TCR triggering ligand aCD3. Nanoarrays were produced by BCML, a well-established technique enabling ordered deposition of AuNPs on solid inorganic supports with tunable interparticle spacing (Figure 1a).[31] The lateral distance between particles, determining the ligand density, was varied from 35 to 150 nm. The resulting particle density had values of approximately 1010−59 AuNPs/μm^2. Substrates were passivated by covalent attachment of a polyethylene glycol (PEG) film to prevent nonspecific protein adsorption to the glass and to ensure subsequent T cell interaction only with the ligands presented on AuNPs.[32] Similar to a previously described method,[33] antibody molecules were immobilized in a site-directed manner by coupling a thiol-NTA (nitrilo-triacetate) linker to AuNPs and loading the NTA group with Ni^{2+} to ensure maximal biological activity. The nickel complex can bind additional proteins with a terminal sequence containing a stretch of six or more histidine residues (His-tag).[34] We used His-tagged antibody-binding protein G to finally couple aCD3-activating antibodies to the gold nanoarrays in an active orientation (Figure 1b). Supported by a previous characterization of protein nanoarrays functionalized in a similar manner,[33,35] evidence suggests that the typical size of AuNPs on arrays produced by BCML (6−8 nm, surrounded by approximately 5 nm thick PEG matrix upon passivation)[32,35a] restricts binding to only one protein molecule per AuNP. However, Protein G contains multiple binding sites for the Fc region of an antibody, implying that the AuNP density on the arrays is a proportional and indicative parameter of aCD3 density on the surface, rather than an absolute value. Prior to nanoarray functionalization, the site-directed NTA-His immobilization strategy was assessed by quartz crystal microbalance with dissipation (QCM-D) on homogeneous gold sensors. Successive binding of all the components was confirmed by the appropriate frequency shifts (Supporting Information Figure 1a). The successful functionalization of gold nanoarrays with aCD3 was verified by fluorescence microscopy (Figure 1c). A clear dipping line separating the functionalized region from the merely passivated part of the substrate can be seen, demonstrating that aCD3 binding is confined to areas decorated with gold nanoparticles;

dx.doi.org/10.1021/nl4022623 | Nano Lett. 2013, 13, 5090−5097

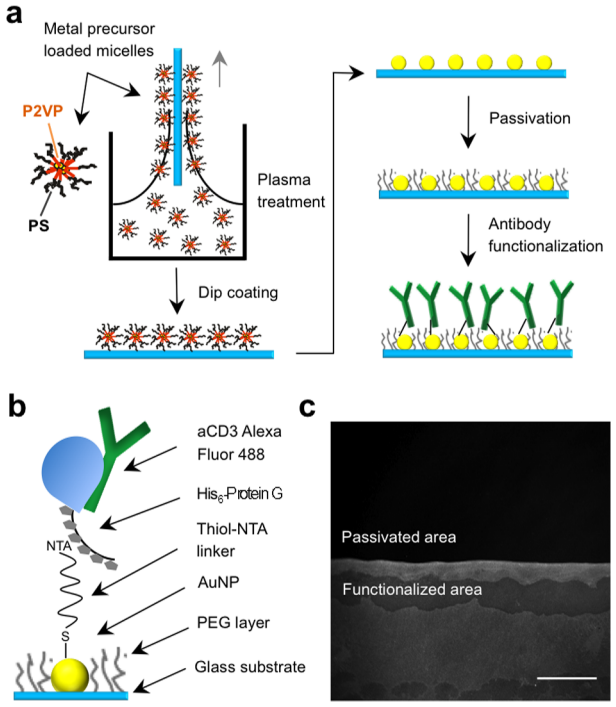

Figure 1. Stimulatory nanoarrays are fabricated by BCML and selective and site-directed protein immobilization techniques. (a) A scheme of stimulatory nanoarray fabrication process including substrate nanopatterning by BCML, passivation, and biofunctionalization. (b) Oriented antibody immobilization on AuNP via thiol-NTA linker and His-tagged Protein G ensures preserved bioactivity on the surface. (c) Fluorescence image of aCD3 AlexaFluor488 nanoarray demonstrating selective functionalization of the nanopatterned area of the substrate, separated from the merely passivated area by a so-called dipping-line (scale bar = 50 μm).

in other words, interaction is prevented in the interparticle areas due to the protein-repellant properties of PEG. Rinsing functionalized nanoarrays with excess imidazole resulted in a decrease in the fluorescent signal close to the PEG background, indicating that the proteins were indeed bound via site-directed NTA-His chemistry to the gold particles (Supporting Information Figure 1c).

To assess the stimulatory potential of aCD3 nanoarrays, we performed several activation read-outs on CD4+ T cells isolated from human peripheral blood of healthy volunteers. CD4+ T cells from healthy donors represent a physiological and clinically relevant target for the proof-of-concept efficiency of stimulatory nanoarrays, although the platform could easily be extended in the future to address the activation of functionally distinct T cell subsets (e.g., Th1, Th2, Th17, and so forth) or antigen-specific T cell clones within this diverse population in a disease-specific context. The cells were cultured on the substrates for 17 h (short-term) or 4 days (long-term) with or without soluble aCD28 as a costimulator. These specific time points were selected based on extensive literature[36−38] that guided our decision on how to best analyze typical T cell activation events that are also relevant for the clinical applications (CD69 surface marker expression, IL-2 production, and proliferation). The first time point (t = 17 h) was set as an early time point when the expression of most of the "classical" activation markers (e.g., CD25 and CD69) and cytokines (e.g., IL-2) have already been induced, but major phenotypic alterations and proliferation have not yet taken place. On the other hand, cell proliferation typically peaks around day 3−4 after polyclonal stimulation with aCD3 mAbs, clarifying the choice of the second time point (t = 4 d).[38] Standard positive and negative controls in 96 well plates were run in parallel to each experiment on nanoarrays. We chose the CD69 antigen as a marker for short-term activation as it is one of the earliest markers to appear on the surface of activated T cells,[36] generally parallels the ensuing proliferative response in vitro, and gives a good estimate of T cell functionality in the clinic.[39] Moreover, CD69 is a well-established activation marker that is virtually undetectable on the plasma membrane of resting T cells but is rapidly and transiently upregulated upon cell stimulation; these facts make it highly suitable for the direct measurement of T cell responses to various experimental stimuli. We found that an aCD3 nanoarray by itself (without additional stimulators) is sufficient to differentially induce CD69 expression on T cells, but successful induction did dependent on interparticle distance (Figure 2a). We proved that CD69 upregulation on nanoarrays was specific to aCD3 by using the matching isotype control mAbs, which immobilized in the same manner but failed to induce any significant response (Supporting Information Figure 3a). Freshly isolated CD4+ T cells cultured without any treatment expressed virtually no CD69 (Supporting Information Figure 3b,c). By decreasing the distance between AuNPs on the array aCD3 density on the surface can be increased, which results in stronger T cell activation in terms of the percentage of CD69 positive cells (Figure 2b,c). The effect was most striking between 100 and 60 nm arrays and CD69 expression reached a high plateau at 60 nm interparticle distance. As expected, providing a costimulatory signal to T cells in the form of soluble aCD28 significantly enhanced T cell activation on all substrates, excluding the high density (35 nm interparticle distance) aCD3 nanoarrays where the difference was noticeable but not significant (p = 0.05) (Figure 2a−c). Providing soluble anti-CD28 to T cells without an established contact with aCD3 did not have any effect on the expression of the CD69 activation marker (Supporting Information Figure 3b).

We next sought to examine the production of IL-2 as an example of a more committed response of T cells to nanoarrays, which is also used to assess lymphocyte function in the clinic. Stimulating T cells solely through contact with an aCD3 nanoarray did not induce meaningful IL-2 production; in other words, IL-2 production was below the sensitivity limit of the cytokine detection assay (Figure 2d,e). Similar results were obtained in control well plates that were homogenously coated with aCD3. Adding soluble aCD28 as a costimulator was a prerequisite to efficiently trigger IL-2 secretion by T cells. These observations are in agreement with the generally accepted two-signal model of lymphocyte activation,[40] which postulates that complete T cell activation requires TCR triggering (signal 1) as well as a second costimulatory signal (signal 2). This allows T cells to produce sufficient amounts of IL-2 and other cytokines necessary for clonal expansion, differentiation, and consequently the generation of an optimal immune response. Without CD28 engagement T cells require high TCR occupancy and prolonged stimulation to accumulate enough activation signal to initiate subsequent processes, but CD28 ligation lowers the threshold for T cell activation.[41] In our system, a threshold for cytokine production could not be reached by signal 1 alone, not even at the highest surface density of the strong TCR-complex agonist aCD3 (Figure 2e). On the other hand, the presence of costimulation led to an

dx.doi.org/10.1021/nl4022623 | Nano Lett. 2013, 13, 5090−5097

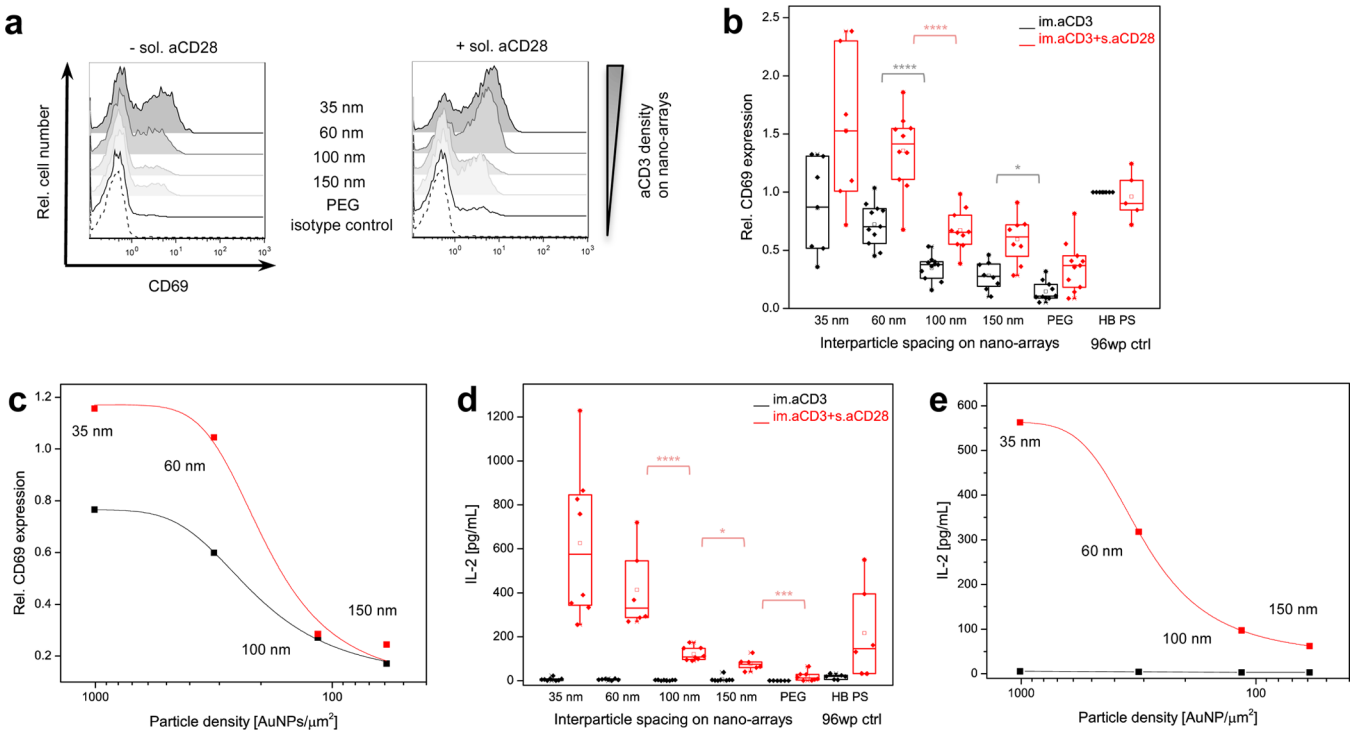

Figure 2. Nanoarrays presenting different densities of aCD3 trigger a differential T cell response that is costimulation dependent, as determined by CD69 upregulation and IL-2 secretion. Freshly isolated CD4+ T cells (10^5/well) were seeded on aCD3 nanoarrays of different spacing or PEG control with or without 2 μg/mL aCD28 as designated, as well as plastic well controls (HB PS = high-binding polystyrene, im. = immobilized, s. = soluble). After 17 h of culture, the cells were analyzed for CD69 expression by anti-CD69PE staining and flow cytometry, while IL-2 concentration was determined in culture supernatants by ELISA. (a) Representative flow cytometric histograms showing relative sizes of activated, CD69 expressing and nonactivated, CD69 negative T cell populations on different surfaces. (b) Box plots summarizing relative CD69 expression (percentage of CD69 positive cells normalized to same parameter on aCD3-coated plastic wells) from independent experiments (n = 6) and (c) corresponding dose–response curve (median values corrected for PEG background). (d) Box plots summarizing IL-2 levels from independent experiments (n = 4) and (e) corresponding dose–response curve (median values corrected for PEG background). Data were analyzed by Kruskal–Wallis ANOVA for multiple comparison and Mann–Whitney U-test for specific sample pairs (*p < 0.05, ** p < 0.01, *** p < 0.005, **** p < 0.001).

incremental increase in the T cell response, similar to the increase of CD69 upregulation observed in response to aCD3 nanoarray density. As observed for CD69 upregulation, we found a sharp increase in IL-2 levels when comparing surfaces with 60 and 100 nm interparticle distance as well as a secretion plateau at an interparticle distance of about 60 nm (Figure 2d). IL-2 production correlated more strongly with aCD3 density than CD69 expression. The idea of including CD28 ligands, in particular aCD28, which does not bind the coinhibitory receptor CTLA-4, on artificial APC systems to achieve long-term expansion of functional T cells in the context of ACT is not new.[42] It has been hypothesized that the mode of CD28 costimulation (soluble vs bound corresponding to trans vs cis presentation on the aCD3 presenting surface) influences the pattern of secreted cytokines and leads to the generation of different T helper cell subsets.[42] In our experiments, we observed maximal responses in terms of both CD69 upregulation and IL-2 production on plastic wells coated with both aCD3 and aCD28 (Supporting Information Figure 4). Therefore, we plan to coimmobilize aCD28 with aCD3 on our next generation of stimulatory nanoarrays. Interestingly, on high density nanoarrays, both the array with 35 nm and the array with 60 nm particle spacing and after addition of soluble costimulator, IL-2 levels were higher compared to the corresponding control consisting of T cells activated by aCD3 and soluble aCD28 plastic bound (Figure 2d). Theoretically, the homogenously coated high-binding surfaces of the plate wells should present much higher numbers of aCD3 molecules, but we hypothesize that due to physisorption a large portion of the bound aCD3 molecules may be in an inactive orientation. Crowding of the antibodies on the surface can also result in steric hindrance, thus preventing efficient TCR triggering. Nevertheless, on aCD3 nanoarrays the antibodies should be securely anchored at binding sites and should be in their active orientation, due to site-directed immobilization on the nanoarray.

aCD3 nanoarrays also support T cell survival on a longer time scale, as can be seen on photomicrographs of cells after 4 days of culturing on the substrates (Figure 3a). Enlarged "blasts" and clusters of activated T cells or elongated cells (with a "uropod-like" structure) can be found on aCD3 nanoarrays with or without addition of soluble aCD28, respectively, but not on PEG controls. Furthermore, we detected more clusters and clusters of bigger diameter on the denser nanoarrays, with 35 and 60 nm particle spacing. Efficient T cell stimulation ultimately leads to efficient cell proliferation, a highly relevant activation event for predicted clinical applications that typically require extensive T cell expansion. Cell proliferation was evaluated after 4 days of culturing on various substrates using the carboxyfluorescein diacetate succinimidyl ester (CFSE)-dilution assay, as previously described.[43] Accurate tracking of cell divisions is possible with this fluorescent dye, because it

dx.doi.org/10.1021/nl4022623 | Nano Lett. 2013, 13, 5090–5097

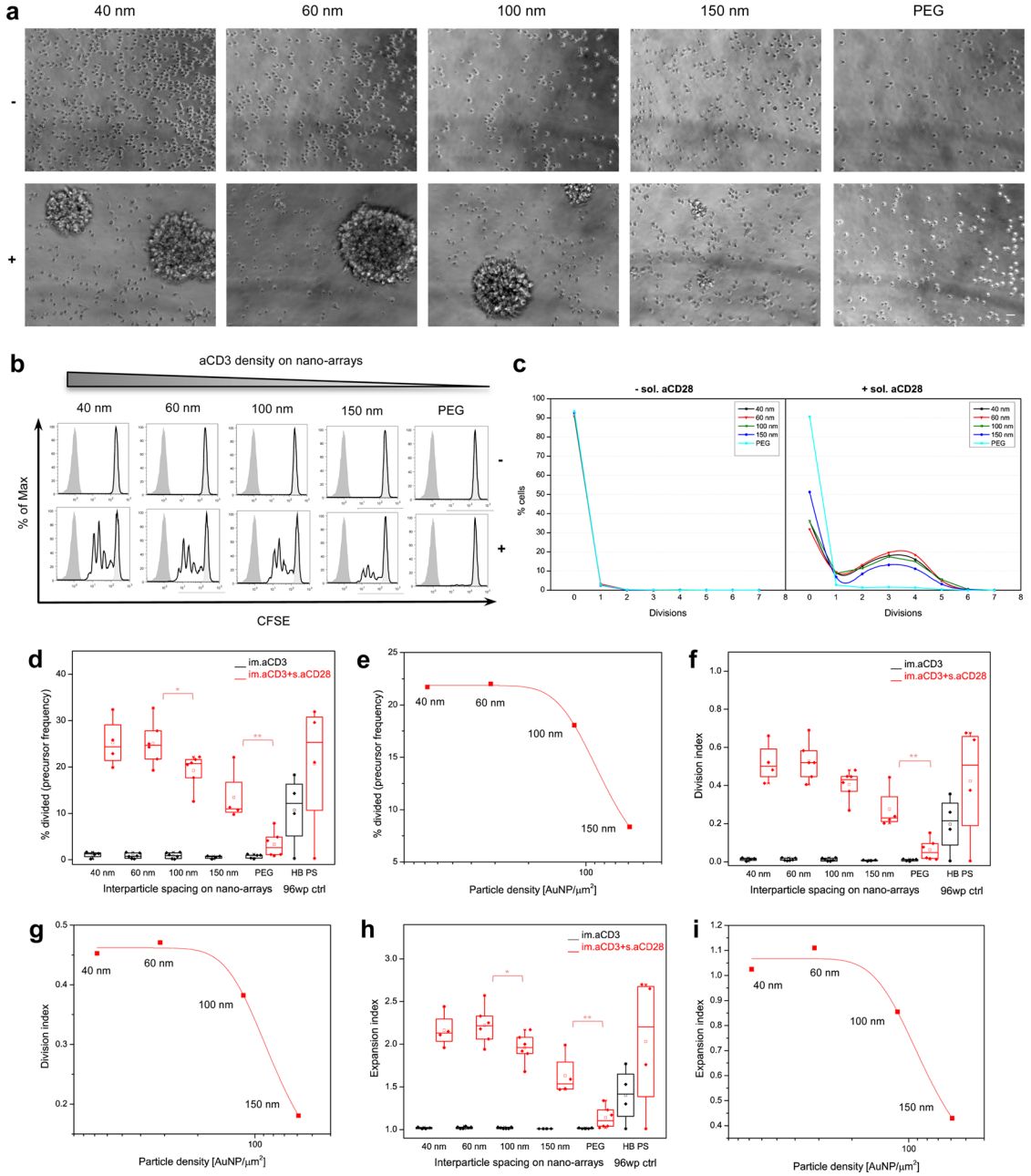

Figure 3. Although aCD3 nanoarrays support long-term T cell survival, costimulation is prerequisite for triggering cell proliferation on substrates. CFSE-labeled CD4+ T cells (5×10^4/well) were cultured for 4 days on aCD3 nanoarrays or PEG controls with (+) or without (−) 2 μg/mL soluble aCD28, as well as plastic well controls (HB PS = high-binding polystyrene, im. = immobilized, s. = soluble). (a) Bright-field images showing typical morphology of T cells observed on different substrates. Elongated cells (with uropod-like structure), T cell blasts, and clusters can be noticed where the surfaces induced activation (scale bar = 20 μm). (b) Representative histograms showing a peak of nondividing cells (light gray) and autofluorescence of nonlabeled cells (dark gray). Each fluorescent peak in between represents a distinct cell population that entered another division. (c) Percentage of cells found in different generations (data shown are median values from three independent experiments) (d,f,h) Box plots indicating different proliferation parameters from three independent experiments (% divided (precursor frequency) = the original fraction of T cells that divided at least once; division index = average numbers of divisions cells have undergone; expansion index = average fold expansion of cell culture) and (e,g,i) corresponding dose−response curves (median values corrected for PEG background). Data were analyzed by Kruskal−Wallis ANOVA for multiple comparison and Mann−Whitney U-test for specific sample pairs (* $p < 0.05$, ** $p < 0.01$, *** $p < 0.005$, **** $p < 0.001$).

partitions equally between dividing cells, thus halving its intensity with every cell division.[44] In this set of experiments, we also found that the induction of cell proliferation also depends on the addition of soluble aCD28 and therefore requires more than only an aCD3 presenting nanoarray (Figure 3b). This dependence on costimulation is not surprising because IL-2 is critical for cell proliferation and the induction of IL-2 secretion was aCD28 dependent in our system. It was discovered that differences in IL-2 production generally reflect differences in T cell proliferation. Differences in specific proliferation parameters between nanoarrays, in comparison, were less distinct than differences in IL-2 secretion (Figure 3c−i). On all nanoarrays that received additional costimulation the majority of cells that divided were in the third or fourth

dx.doi.org/10.1021/nl4022623 | Nano Lett. 2013, 13, 5090−5097

generation, although a significant amount of cells (30−50%) remained undivided (Figure 3c). On high-density aCD3 nanoarrays with 40 and 60 nm particle spacing, the original T cell fraction that entered proliferation (precursor frequency) was around 25% (Figure 3d,e) and the whole T cell culture underwent an average of 0.5 divisions (Figure 3f−g) and 2.2-fold expansion (Figure 3h,i). On 150 nm arrays, these numbers decreased significantly to 10% precursor frequency, 0.2 divisions, and 1.5-fold expansion.

At the present time, we have not directly assessed the long-term chemical stability of our stimulatory platform, as our data clearly show that it is biologically functional. All measured T cell responses showed a strong positive correlation with aCD3 density with a density threshold below ∼59 AuNPs/μm^2 (150 nm nanoarrays). Importantly, the fact that T cell responses on the high-density aCD3 nanoarrays were significantly stronger compared to the response in the aCD3-absorbed plastic dishes, clearly indicates improved efficiency of our system compared to current conventional approaches. At the theoretical level, possible long-term instability of our stimulatory platform could include partial disruption of the PEG layer and aCD3 dissociation from AuNPs due to His-NTA lability or binding of adhesion associated matrix molecules from the media to the PEG free area. Redistribution of dissociated aCD3 on exposed glass is unlikely due to the presence of a large liquid reservoir, making the loss of aCD3 quite possible. Still, this could affect the overall aCD3 density and adhesive background presented to T cells at later time points. However, extensive literature on in vitro activation dynamics of T cells, as well as in vivo studies of T cell interaction with dendritic cells (which our novel in vitro stimulation system aims to mimic), suggest that efficient T cell activation may be achieved by stable contacts with stimulatory interfaces of only few hours up to 16 h[45] and that these initial phases of activation are determining the outcome of the cellular response. Thus, as suggested by the literature, any deterioration of stimulatory nanoarrays would critically affect T cell activation only during the first 16 h of culturing. Our present data showing efficient T cell activation on the appropriately functionalized nanoarrays suggest that the platform is very likely stable for this time frame. Therefore, initial surface conditions are precisely defined by ligand nanopatterning, stable within the time frame relevant for efficient T cell activation and determine the long-term cellular behavior, as the cells still respond differently on nanoarrays of various spacing after 4 days of culturing. Indeed, there is still room for improvement in stimulatory nanoarray design and future studies could address this issue by testing more stable immobilization strategies[46] and robust PEG hydrogels as passivation matrices.[47] Such "enhanced" aCD3 nanoarrays might lead to an even stronger T cell response in the future, as well as enable additional aspects of T cell activation (e.g., mechanosensing) to be investigated.

Although quantitative events like signal strength play an important role in T cell activation and differentiation, the optimization and standardization of stimulatory platforms employed to tackle immunological questions still requires serious attention.[48] To vary TCR signal strength, it is common to use serial dilutions of aCD3 as the stimulatory substrate in the coating solution applied to traditional plastic plates. The amount of functional, bound mAbs in this case is very difficult to estimate due to the different binding capacities of available plastics and the occurrence of random antibody orientation by physisorption. Physisorption can thereby render a significant portion of antibodies on the surface inactive. In earlier generations of stimulatory beads, antibodies were commonly attached by simple adsorption on latex beads or covalent coupling via amine groups to magnetic beads.[7] Direct chemical immobilizations of antibodies can also impair their functionality on the surface. Commercially available magnetic beads, considered to be the golden standard in T cell expansion, are currently improving antibody surface activity by indirect coupling strategies via anti-IgG antibody (Dynal) or anti-biotin antibody (Miltenyi). (However, biotin is usually introduced at random sites and cannot guarantee specific antibody orientation.) A common approach to tuning signal strength when stimulating T cells with magnetic beads is to vary bead-to-cell ratio.[49] However, by doing this, the local amount of aCD3 presented to each T cells remains more-or-less constant, as all beads are functionalized with the same antibody concentration. Previous work with latex beads has highlighted the importance of a continuous large surface area for efficient T cell stimulation and the existence of a critical bead size of 5 μm, under which the T cell response significantly decreases. This decrease cannot be compensated by using a larger number of smaller beads (and thereby increasing the overall ligand density).[50] It is, therefore, important to be able to control local antibody density on the stimulatory substrate. Our system is unique for several reasons: (1) it has fixed nanoscale areas for aCD3 binding, which are predetermined by AuNPs embedded in a passivated PEG matrix and (2) it is able to fine-tune local ligand density by varying the distance between aCD3 bearing AuNPs.

In conclusion, we developed stimulatory substrates presenting different aCD3 nanoscale densities by self-assembled nanopatterning in combination with selective and site-directed protein immobilization techniques. aCD3 nanoarrays by themselves were able to trigger early molecular activation events in T cells in the form of moderate CD69 upregulation, but costimulation with soluble aCD28 was mandatory for achieving relevant and productive cellular responses like IL-2 secretion and T cell proliferation. In all assessed activation read-outs, the T cell response showed a strong correlation with aCD3 density on the nanoarrays. Higher activation was achieved on higher density arrays (those with less interparticle distance). Cellular responses reached a plateau at 60 nm interparticle distance (316 AuNPs/μm^2) and declined significantly between an interparticle spacing of 60 and 100 nm. On the basis of observations from dose−response curves, a potential density threshold has been determined at around or under 59 AuNPs/μm^2 (150 nm nanoarrays). T cell responses on traditional aCD3-absorbed plastic dishes were lower than on high-density nanopatterned substrates, which indicates an enhanced efficiency of stimulatory nanopatterned substrates compared to conventional cell culture substrates. The developed aCD3 nanoarrays may be applicable as APC surrogates with a molecularly and spatially controllable and consistent surface for fine modulation of desired T cell responses. In the future, they may be useful in achieving an optimal clinical outcome during ACT.

■ ASSOCIATED CONTENT

Ⓢ Supporting Information

Materials and methods, transforming interparticle spacing to particle density on nanoarrays, probing the site-directed immobilization strategy on homogeneous gold and gold nanoarrays, cell morphology on substrates after 17 h, specificity

dx.doi.org/10.1021/nl4022623 | Nano Lett. 2013, 13, 5090−5097

of CD69 upregulation by aCD3 on nanoarrays and specific stimuli in general, costimulation dependence of IL-2 secretion, long-term T cell survival and proliferation in control samples. This material is available free of charge via the Internet at http://pubs.acs.org.

AUTHOR INFORMATION

Corresponding Author

*E-mail: spatz@is.mpg.de.

Author Contributions

J.M. performed the experiments. J.M. and J.P.S. are responsible for the conceptual design of the experiments. The manuscript was written with contributions from all authors. All authors have given approval to the final version of the manuscript.

Notes

The authors declare no competing financial interest.

ACKNOWLEDGMENTS

The authors would like to thank Christine Belz and Nina Grunze for helpful discussion and corrections. The experimental work was generously financially supported by the Heinrich-Lohstöter Foundation. The Max Planck Society is acknowledged for financial support. The work was part of the European Union Seventh Framework Program (FP7/2007-2013) under Grant NMP4-LA-2009-229289 NanoII. This work is also part of the excellence cluster CellNetwork at the University of Heidelberg. J.P.S. is the Weston Visiting Professor at the Weizmann Institute of Science.

ABBREVIATIONS

ACT, adoptive cell therapy; BCML, block copolymer micellar nanolithograpgy; AuNP, gold nanoparticle; aCD3, anti-CD3 antibody; aCD28, anti-CD28 antibody; CD69, cluster of differentiation 69; IL-2, interleukin-2; CFSE, carboxyfluoresceindiacetatesuccinimidyl ester

REFERENCES

(1) June, C. H. Adoptive T cell therapy for cancer in the clinic. *J. Clin. Invest.* **2007**, *117* (6), 1466−1476.

(2) June, C. H. Principles of adoptive T cell cancer therapy. *J. Clin. Invest.* **2007**, *117* (5), 1204−12.

(3) Germain, R. N. MHC-dependent antigen processing and peptide presentation: Providing ligands for T lymphocyte activation. *Cell* **1994**, *76* (2), 287−299.

(4) Altman, A.; Mark Coggeshall, K.; Mustelin, T. Molecular events mediating T cell activation. *Adv. Immunol.* **1990**, *48*, 227−360.

(5) Kim, J. V.; Latouche, J.-B.; Riviere, I.; Sadelain, M. The ABCs of artificial antigen presentation. *Nat. Biotechnol.* **2004**, *22* (4), 403−410.

(6) Platzman, I.; Janiesch, J.-W.; Matić, J.; Spatz, J. P. Artificial Antigen-Presenting Interfaces in the Service of Immunology. *Isr. J. Chem.* **2013**, DOI: 10.1002/ijch.201300060.

(7) Steenblock, E. R.; Wrzesinski, S. H.; Flavell, R. A.; Fahmy, T. M. Antigen presentation on artificial acellular substrates: modular systems for flexible, adaptable immunotherapy. *Exp. Opin. Biol. Ther.* **2009**, *9* (4), 451−464.

(8) Steenblock, E. R.; Fahmy, T. M. A Comprehensive Platform for Ex Vivo T-cell Expansion Based on Biodegradable Polymeric Artificial Antigen-presenting Cells. *Mol .Ther.* **2008**, *16* (4), 765−772.

(9) Platzman, I.; Janiesch, J. W.; Spatz, J. P. Synthesis of nanostructured and biofunctionalized water-in-oil droplets as tools for homing T cells. *J. Am. Chem. Soc.* **2013**, *135* (9), 3339−42.

(10) Irvine, D. J.; Doh, J. Synthetic surfaces as artificial antigen presenting cells in the study of T cell receptor triggering and immunological synapse formation. *Semin. Immunol.* **2007**, *19* (4), 245−254.

(11) (a) Acuto, O.; Michel, F. CD28-mediated co-stimulation: a quantitative support for TCR signalling. *Nat. Rev. Immunol.* **2003**, *3* (12), 939−951. (b) Frauwirth, K. A.; Thompson, C. B. Activation and inhibition of lymphocytes by costimulation. *J. Clin. Invest.* **2002**, *109* (3), 295−299. (c) Sharpe, A. H.; Freeman, G. J. The B7-CD28 superfamily. *Nat. Rev. Immunol.* **2002**, *2* (2), 116−26.

(12) Hosseini, B. H.; Louban, I.; Djandji, D.; Wabnitz, G. H.; Deeg, J.; Bulbuc, N.; Samstag, Y.; Gunzer, M.; Spatz, J. P.; Hammerling, G. J. Immune synapse formation determines interaction forces between T cells and antigen-presenting cells measured by atomic force microscopy. *Proc Natl Acad Sci U S A* **2009**, *106* (42), 17852−7.

(13) Lanzavecchia, A.; Sallusto, F. Progressive differentiation and selection of the fittest in the immune response. *Nat. Rev. Immunol.* **2002**, *2* (12), 982−987.

(14) Andersen, P. S.; Menné, C.; Mariuzza, R. A.; Geisler, C.; Karjalainen, K. A Response Calculus for Immobilized T Cell Receptor Ligands. *J. Biol. Chem.* **2001**, *276* (52), 49125−49132.

(15) (a) Iezzi, G.; Karjalainen, K.; Lanzavecchia, A. The Duration of Antigenic Stimulation Determines the Fate of Naive and Effector T Cells. *Immunity* **1998**, *8* (1), 89−95. (b) Gett, A. V.; Sallusto, F.; Lanzavecchia, A.; Geginat, J. T cell fitness determined by signal strength. *Nat. Immunol.* **2003**, *4* (4), 355−360.

(16) Lanzavecchia, A.; Sallusto, F. Understanding the generation and function of memory T cell subsets. *Curr. Opin. Immunol.* **2005**, *17* (3), 326−332.

(17) (a) Paul, W. E. What determines Th2 differentiation, in vitro and in vivo? *Immunol. Cell Biol.* **2010**, *88* (3), 236−9. (b) Paul, W. E.; Zhu, J. How are TH2-type immune responses initiated and amplified? *Nat. Rev. Immunol.* **2010**, *10* (4), 225−235.

(18) Purvis, H. A.; Stoop, J. N.; Mann, J.; Woods, S.; Kozijn, A. E.; Hambleton, S.; Robinson, J. H.; Isaacs, J. D.; Anderson, A. E.; Hilkens, C. M. Low-strength T-cell activation promotes Th17 responses. *Blood* **2010**, *116* (23), 4829−37.

(19) (a) Turner, M. S.; Kane, L. P.; Morel, P. A. Dominant role of antigen dose in CD4+Foxp3+ regulatory T cell induction and expansion. *J. Immunol.* **2009**, *183* (8), 4895−903. (b) Long, S. A.; Rieck, M.; Tatum, M.; Bollyky, P. L.; Wu, R. P.; Muller, I.; Ho, J. C.; Shilling, H. G.; Buckner, J. H. Low-dose antigen promotes induction of FOXP3 in human CD4+ T cells. *J. Immunol.* **2011**, *187* (7), 3511−20.

(20) Badou, A.; Savignac, M.; Moreau, M.; Leclerc, C.; Foucras, G.; Cassar, G.; Paulet, P.; Lagrange, D.; Druet, P.; Guéry, J.-C.; Pelletier, L. Weak TCR stimulation induces a calcium signal that triggers IL-4 synthesis, stronger TCR stimulation induces MAP kinases that control IFN-γ production. *Eur. J. Immunol.* **2001**, *31* (8), 2487−2496.

(21) (a) Restifo, N. P.; Dudley, M. E.; Rosenberg, S. A. Adoptive immunotherapy for cancer: harnessing the T cell response. *Nat. Rev. Immunol.* **2012**, *12* (4), 269−281. (b) Gattinoni, L.; Klebanoff, C. A.; Restifo, N. P. Paths to stemness: building the ultimate antitumour T cell. *Nat. Rev. Cancer* **2012**, *12* (10), 671−84. (c) Gattinoni, L.; Powell, D. J., Jr.; Rosenberg, S. A.; Restifo, N. P. Adoptive immunotherapy for cancer: building on success. *Nat. Rev. Immunol.* **2006**, *6* (5), 383−93. (d) Hinrichs, C. S.; Gattinoni, L.; Restifo, N. P. Programming CD8+ T cells for effective immunotherapy. *Curr. Opin. Immunol.* **2006**, *18* (3), 363−70.

(22) Mossman, K. D.; Campi, G.; Groves, J. T.; Dustin, M. L. Altered TCR Signaling from Geometrically Repatterned Immunological Synapses. *Science* **2005**, *310* (5751), 1191−1193.

(23) Giannoni, F.; Barnett, J.; Bi, K.; Samodal, R.; Lanza, P.; Marchese, P.; Billetta, R.; Vita, R.; Klein, M. R.; Prakken, B.; Kwok, W. W.; Sercarz, E.; Altman, A.; Albani, S. Clustering of T Cell Ligands on Artificial APC Membranes Influences T Cell Activation and Protein Kinase C θ Translocation to the T Cell Plasma Membrane. *J. Immunol.* **2005**, *174* (6), 3204−3211.

(24) Fadel, T. R.; Look, M.; Staffier, P. A.; Haller, G. L.; Pfefferle, L. D.; Fahmy, T. M. Clustering of Stimuli on Single-Walled Carbon Nanotube Bundles Enhances Cellular Activation. *Langmuir* **2009**, *26* (8), 5645−5654.

(25) (a) Doh, J.; Irvine, D. J. Immunological synapse arrays: patterned protein surfaces that modulate immunological synapse structure formation in T cells. *Proc. Natl. Acad. Sci. U.S.A.* **2006**, *103* (15), 5700−5. (b) Shen, K.; Thomas, V. K.; Dustin, M. L.; Kam, L. C. Micropatterning of costimulatory ligands enhances CD4+ T cell function. *Proc. Natl. Acad. Sci. U.S.A.* **2008**, *105* (22), 7791−6.

(26) (a) Schamel, W. W.; Arechaga, I.; Risueno, R. M.; van Santen, H. M.; Cabezas, P.; Risco, C.; Valpuesta, J. M.; Alarcon, B. Coexistence of multivalent and monovalent TCRs explains high sensitivity and wide range of response. *J. Exp. Med.* **2005**, *202* (4), 493−503. (b) Molnar, E.; Swamy, M.; Holzer, M.; Beck-Garcia, K.; Worch, R.; Thiele, C.; Guigas, G.; Boye, K.; Luescher, I. F.; Schwille, P.; Schubert, R.; Schamel, W. W. A. Cholesterol and Sphingomyelin Drive Ligand-independent T-cell Antigen Receptor Nanoclustering. *J. Biol. Chem.* **2012**, *287* (51), 42664−42674. (c) Lillemeier, B. F.; Mortelmaier, M. A.; Forstner, M. B.; Huppa, J. B.; Groves, J. T.; Davis, M. M. TCR and Lat are expressed on separate protein islands on T cell membranes and concatenate during activation. *Nat. Immunol.* **2010**, *11* (1), 90−96.

(27) Cavalcanti-Adam, E. A.; Volberg, T.; Micoulet, A.; Kessler, H.; Geiger, B.; Spatz, J. P. Cell Spreading and Focal Adhesion Dynamics Are Regulated by Spacing of Integrin Ligands. *Biophys. J.* **2007**, *92* (8), 2964−2974.

(28) Thelen, K.; Wolfram, T.; Maier, B.; Jährling, S.; Tinazli, A.; Piehler, J.; Spatz, J. P.; Pollerberg, G. E. Cell adhesion molecule DM-GRASP presented as nanopatterns to neurons regulates attachment and neurite growth. *Soft Matter* **2007**, *3* (12), 1486−1491.

(29) Ranzinger, J.; Krippner-Heidenreich, A.; Haraszti, T.; Bock, E.; Tepperink, J.; Spatz, J. P.; Scheurich, P. Nanoscale Arrangement of Apoptotic Ligands Reveals a Demand for a Minimal Lateral Distance for Efficient Death Receptor Activation. *Nano Lett.* **2009**, *9* (12), 4240−4245.

(30) (a) Heller, K. N.; Gurer, C.; Münz, C.. Virus-specific CD4+ T cells: ready for direct attack. *J. Exp. Med.* **2006**, *203* (4), 805−808. (b) Muranski, P.; Restifo, N. P. Adoptive immunotherapy of cancer using CD4(+) T cells. *Curr. Opin. Immunol.* **2009**, *21* (2), 200−8.

(31) Spatz, J. P.; Mössmer, S.; Hartmann, C.; Möller, M.; Herzog, T.; Krieger, M.; Boyen, H.-G.; Ziemann, P.; Kabius, B. Ordered Deposition of Inorganic Clusters from Micellar Block Copolymer Films. *Langmuir* **1999**, *16* (2), 407−415.

(32) Blümmel, J.; Perschmann, N.; Aydin, D.; Drinjakovic, J.; Surrey, T.; Lopez-Garcia, M.; Kessler, H.; Spatz, J. P. Protein repellent properties of covalently attached PEG coatings on nanostructured SiO_2-based interfaces. *Biomaterials* **2007**, *28* (32), 4739−4747.

(33) Aydin, D.; Schwieder, M.; Louban, I.; Knoppe, S.; Ulmer, J.; Haas, T. L.; Walczak, H.; Spatz, J. P. Micro-nanostructured protein arrays: a tool for geometrically controlled ligand presentation. *Small* **2009**, *5* (9), 1014−8.

(34) Sigal, G. B.; Bamdad, C.; Barberis, A.; Strominger, J.; Whitesides, G. M. A self-assembled monolayer for the binding and study of histidine-tagged proteins by surface plasmon resonance. *Anal. Chem.* **1996**, *68* (3), 490−7.

(35) (a) Wolfram, T.; Belz, F.; Schoen, T.; Spatz, J. P. Site-specific presentation of single recombinant proteins in defined nanoarrays. *Biointerphases* **2007**, *2* (1), 44−48. (b) Aydin, D.; Louban, I.; Perschmann, N.; Blümmel, J.; Lohmüller, T.; Cavalcanti-Adam, E. A.; Haas, T. L.; Walczak, H.; Kessler, H.; Fiammengo, R.; Spatz, J. P. Polymeric Substrates with Tunable Elasticity and Nanoscopically Controlled Biomolecule Presentation. *Langmuir* **2010**, *26* (19), 15472−15480. (c) Groll, J.; Albrecht, K.; Gasteier, P.; Riethmueller, S.; Ziener, U.; Moeller, M. Nanostructured Ordering of Fluorescent Markers and Single Proteins on Substrates. *ChemBioChem* **2005**, *6* (10), 1782−1787.

(36) Caruso, A.; Licenziati, S.; Corulli, M.; Canaris, A. D.; De Francesco, M. A.; Fiorentini, S.; Peroni, L.; Fallacara, F.; Dima, F.; Balsari, A.; Turano, A. Flow cytometric analysis of activation markers on stimulated T cells and their correlation with cell proliferation. *Cytometry* **1997**, *27* (1), 71−76.

(37) Reddy, M.; Eirikis, E.; Davis, C.; Davis, H. M.; Prabhakar, U. Comparative analysis of lymphocyte activation marker expression and cytokine secretion profile in stimulated human peripheral blood mononuclear cell cultures: an in vitro model to monitor cellular immune function. *J. Immunol. Methods* **2004**, *293* (1,Äì2), 127−142.

(38) Muul, L. M.; Silvin, C.; James, S. P.; Candotti, F. Measurement of proliferative responses of cultured lymphocytes. *Curr. Protoc. Immunol.* **2008**, Chapter 7, Unit 7 10 1−7 10 24.

(39) (a) Nielsen; Afzelius; ErsbØll; Hansen. Expression of the activation antigen CD69 predicts functionality of in vitro expanded peripheral blood mononuclear cells (PBMC) from healthy donors and HIV-infected patients. *Clin. Exp. Immunol.* **1998**, *114* (1), 66−72. (b) Lindsey, W.; Lowdell, M.; Marti, G.; Abbasi, F.; Zenger, V.; King, K.; Lamb, L. CD69 expression as an index of T-cell function: assay standardization, validation and use in monitoring immune recovery. *Cytotherapy* **2007**, *9* (2), 123−132.

(40) (a) Bretscher, P. The two-signal model of lymphocyte activation twenty-one years later. *Immunol. Today* **1992**, *13* (2), 74−76. (b) June, C. H.; Bluestone, J. A.; Nadler, L. M.; Thompson, C. B. The B7 and CD28 receptor families. *Immunol. Today* **1994**, *15* (7), 321−331.

(41) Viola, A.; Lanzavecchia, A.; Cell, T. Activation Determined by T Cell Receptor Number and Tunable Thresholds. *Science* **1996**, *273* (5271), 104−106.

(42) Levine, B. L.; Bernstein, W. B.; Connors, M.; Craighead, N.; Lindsten, T.; Thompson, C. B.; June, C. H. Effects of CD28 costimulation on long-term proliferation of CD4+ T cells in the absence of exogenous feeder cells. *J. Immunol.* **1997**, *159* (12), 5921−30.

(43) Nagar, M.; Jacob-Hirsch, J.; Vernitsky, H.; Berkun, Y.; Ben-Horin, S.; Amariglio, N.; Bank, I.; Kloog, Y.; Rechavi, G.; Goldstein, I. TNF Activates a NF-κB−Regulated Cellular Program in Human $CD45RA^-$ Regulatory T Cells that Modulates Their Suppressive Function. *J. Immunol.* **2010**, *184* (7), 3570−3581.

(44) Lyons, A. B.; Parish, C. R. Determination of lymphocyte division by flow cytometry. *J. Immunol. Methods* **1994**, *171* (1), 131−137.

(45) Dustin, M. L. A dynamic view of the immunological synapse. *Semin. Immunol.* **2005**, *17* (6), 400−10.

(46) Wegner, S. V.; Spatz, J. P. Cobalt(III) as a Stable and Inert Mediator Ion between NTA and His6-Tagged Proteins. *Angew. Chem., Int. Ed.* **2013**, DOI: 10.1002/anie.201210317.

(47) Graeter, S. V.; Huang, J.; Perschmann, N.; López-García, M.; Kessler, H.; Ding, J.; Spatz, J. P. Mimicking Cellular Environments by Nanostructured Soft Interfaces. *Nano Lett.* **2007**, *7* (5), 1413−1418.

(48) O'Garra, A.; Gabrysova, L.; Spits, H. Quantitative events determine the differentiation and function of helper T cells. *Nat. Immunol.* **2011**, *12* (4), 288−294.

(49) Kalamasz, D.; Long, S. A.; Taniguchi, R.; Buckner, J. H.; Berenson, R. J.; Bonyhadi, M. Optimization of Human T-Cell Expansion Ex Vivo Using Magnetic Beads Conjugated with Anti-CD3 and Anti-CD28 Antibodies. *J. Immunother.* **2004**, *27* (5), 405−418.

(50) Mescher, M. Surface contact requirements for activation of cytotoxic T lymphocytes. *J. Immunol.* **1992**, *149* (7), 2402−2405.